Modeling of Marginal Cost for PV Inverter Ancillary Services Considering Inverter Aging under Transactive Energy Framework

Yunting Liu[1], Paychuda Kritprajun[1], Leon M. Tolbert[1,2], Jiaojiao Dong[1], Lin Zhu[1], Joshua C. Hambrick[2], Kevin Schneider[3], Bishnu P. Bhattarai[3]

[1] The University of Tennessee, Knoxville, TN, USA
[2] Oak Ridge National Laboratory, Oak Ridge, TN, USA
[3] Pacific Northwest National Laboratory, Richland, WA, USA
yliu193@utk.edu; pkritpra@vols.utk.edu; tolbert@utk.edu; jdong7@utk.edu; lzhu12@utk.edu; hambrickjc@ornl.gov; kevin.schneider@pnnl.gov; Bishnu.Bhattarai@pnnl.gov

***Abstract* — PV inverters can provide ancillary services while simultaneously providing active power. A transactive energy system (TES) incentivizes a PV inverter to provide ancillary services and compensates for the cost of additional power losses due to additional reactive power production. However, providing ancillary services can shorten the lifetime of the PV inverter since additional reactive power increases the thermal stress of it. This paper models the lifetime shortening effect of a PV inverter when providing ancillary services. Based on the lifetime estimation, an improved marginal cost curve of reactive power generation for the PV inverter is proposed. The improved marginal cost considers the normalized lifetime (NLT) of the PV inverter given the active power, reactive power, and ambient temperature. The proposed NLT algorithm is validated by a simulation case study.**

***Index Terms*—Transactive energy system (TES), PV inverter, inverter aging, ancillary services, supply curve.**

I. Introduction

Solar photovoltaic (PV) integration requires power electronic inverters to interface with the power grid. Many literature have reported that the power electronic devices have shorter lifetime compared to their associated PV panels [1], [2]. Due to the short lifetime of inverters, more than one half of the maintenance cost of a PV system may be attributed to the inverters [3]. In addition, the utility power industry usually expects a long lifetime of inverters so that the inverters could retire from the power grid together with the whole PV system [4].

The failure mechanisms of inverters are complex. Semiconductors and capacitors are the most vulnerable components that lead to inverter failure [4]. Both capacitors and semiconductors are sensitive to temperature [5].

Many power electronic literature have proposed solutions to extend the lifetime of inverters. Andresen *et al*. [6] proposed a maximum-power-point-tracker (MPPT) control for PV systems which limits the maximum junction temperature of the power semiconductors. Yang *et al*. [7], [8] also proposed a MPPT to limit the maximum operating point which will limit temperature indirectly. PV inverter manufacturers design their products by derating the output power as ambient temperature increases [9]–[11].

The transactive energy system (TES) is a concept for distributed systems or microgrid operation to engage more distributed energy resources (DERs), especially non-utility owned DERs connected to the power grid [12]–[15]. The basic idea of TES is to provide an incentive to customers to engage the support from non-utility owned DERs. A double-auction method is applied to determine the cleared price of a bidding. When power generation is sufficient, suppliers can offer low-cost electricity, which encourages customers to buy more electricity [12], [13]. The customer could also offer a low price to purchase electricity if the power demand from the customer is not urgent [16]. TES considers the cost of electricity to optimize its control strategy. This feature can be used to consider the cost of maintaining the PV inverter aging.

Alam *et al*. [12], [13] proposed a transactive approach to engage DERs to provide ancillary services. The bidding strategy considers the extra power loss of the inverter when providing the reactive power and the cost of curtailing the active power to leave room for reactive power production.

Some literature have indicated that the engagement of DERs to provide ancillary services may have negative effect on the lifetime of DER inverters due to the increasing thermal stress [17], [18]. In that case, it may increase the maintenance cost of PV inverters, which will also increase the overall PV energy cost.

This paper proposes a marginal cost model for PV inverters to provide ancillary services considering the aging effect of additional reactive power production. The proposed marginal cost model can effectively avoid excessive thermal stress on the

This work was primarily supported by U.S. Department of Energy Grid Modernization Lab Consortium. This work also made use of Engineering Research Center shared facilities supported by the Engineering Research Center Program of the National Science Foundation and the Department of Energy under NSF Award Number [EEC-1041877] and the CURENT Industry Partnership Program.

PV inverters by offering a higher price when providing ancillary services. Therefore, the lifetime of the PV inverter could be extended. This paper is organized as follows. Section II formulates the power loss of PV inverters. Section III converts the power loss of the PV inverter into a thermal model. Section IV discusses the lifetime estimation of PV inverters. Section V derives the proposed marginal cost of a PV inverter considering the aging effect of additional ancillary services. A case study is provided in Section VI to verify the effectiveness of the proposed marginal cost model.

II. PV Inverter Power Loss Assessment

Power losses of PV inverters mainly come from 1) semiconductor switching loss; 2) semiconductor conduction loss; 3) bulky passive components (dc-link capacitor, filtering inductor, high frequency transformer) power loss; 4) auxiliary circuits (gate drive, controller, EMI filter, sensing circuit) energy consumption. Among the four categories, 1) and 2) dominate at medium to heavy load. The auxiliary circuit energy consumption dominates at light load. Other power losses of PV inverters will not be considered in this paper because they do not have significant contributions to temperature rise.

A. Semiconductor Switching Loss

For a given metal–oxide–semiconductor field-effect transistor (MOSFET) or insulated-gate bipolar transistor (IGBT) of a PV inverter, the switching loss could be formulated as follows [19],

$$P_{sw} = V_{dc} i_s \cdot \frac{1}{2} t_{tot} \cdot f_{sw} \tag{1}$$

where t_{tot} is the total time of current rising/falling and voltage falling/rising when power switches turn on/off. f_{sw} is the switching frequency. t_{tot} is a fixed value once a specific switching device is selected. V_{dc} is the dc-link voltage. i_s is the load current. The switching loss at a turn-on state is shown in Fig. 1 [19].

From (1), the switching loss is proportional to i_s. Since apparent power $S = V_s I_s$ is also proportional to i_s, the switching loss is proportional to S.

$$P_{sw} = k_1 S \tag{2}$$

The coefficient k_1 depends on t_{tot}, f_{sw}, V_{dc}, and the number of devices. Once a PV inverter is assembled, k_1 is a fixed number.

B. Semiconductor Conduction Loss

For the MOSFETs/IGBTs of a PV inverter, the conduction loss could be formulated as follows [19],

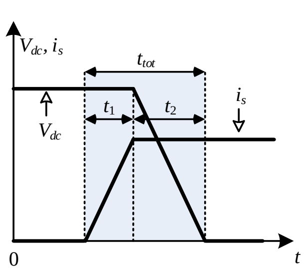

Fig. 1. Switching loss at turn-on state.

$$P_{con} = i_s^2 R_{ds(on)} \tag{3}$$

where $R_{ds(on)}$ is the drain-source on-resistance. It can be seen from (3) that the conduction loss is proportional to i_s^2. Therefore, the conduction loss is proportional to S^2,

$$P_{con} = k_2 S^2 \tag{4}$$

The coefficient k_2 depends on $R_{ds(on)}$, and the number of devices. Once a PV inverter is assembled, k_2 is a fixed number.

C. Auxiliary Circuit Energy Consumption

The auxiliary circuits include gate drive, controller, EMI filter, sensing circuit, etc. The energy consumption of these circuits is independent from the load. Auxiliary circuit energy consumption is fixed once the PV inverter is assembled. The power loss of auxiliary circuits can be formulated as follows,

$$P_{aux} = k_3 \tag{5}$$

The power loss of PV inverter could be formulated as,

$$P_{loss} = P_{sw} + P_{con} + P_{aux} = k_2 S^2 + k_1 S + k_3 \tag{6}$$

The power loss model can be estimated by reviewing the datasheet provided by the manufacturers, or a more accurate approach is to conduct field tests.

III. Electrothermal Model of PV Inverter

A typical IGBT module with thermal management is shown in Fig. 2 [20]. IGBT and diode chips are the heat source. The junction temperature T_{junc} will be passed to the case of IGBT module through several layers of materials and finally result in case temperature T_c. The case of an IGBT normally will be attached to a heat sink by thermal paste. Thermal paste and heat sink usually have a good thermal conductivity. The resulting heat sink temperature is T_h. The heat sink dissipates the heat to the ambient by convection. Other types of thermal management systems include fans, cold plate, and water cooling.

The Foster thermal model [18] is used to estimate the thermal stress of a PV inverter. The Foster thermal model describes the temperature transient of an object by a branch of RC network. The detailed thermal model of a PV inverter is shown in Fig. 3. The switching loss and conduction loss are the heat source for each IGBT module. In a PV inverter, it normally contains 6 to 8 IGBTs depending on the topology. Each IGBT is attached to the heat sink by thermal paste. The capacitor power loss is the heat source for capacitor. Each PV inverter normally contains several capacitors on the dc link and their thermal resistances are thermally in parallel. The capacitors and other auxiliary circuits such as PCB boards, filtering inductors, EMI filters might not have thermal management depending on inverter design.

Many manufacturers provide the Foster thermal model for their products. The junction temperature of an IGBT module can be formulated as (7), where $1 \le i \le k$, k is the number of IGBTs in a PV inverter; and $1 \le j \le l$, where l is the number of terms in the Foster thermal model. The temperature of the capacitors and auxiliary circuits can also be formulated similar to (7). The derivation is omitted in this paper.

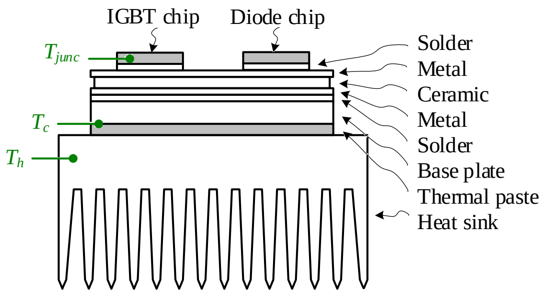

Fig. 2. Typical IGBT module with thermal management.

The PV inverter thermal model can be simplified as shown in Fig.4 since the thermal resistances of the capacitor and auxiliary circuits are typically much greater than that of IGBT modules. The equivalent thermal impedance of PV inverter is

$$Z_{eq} = \sum Z_{IGBT} \parallel Z_{Diode} + \sum Z_{paste} + Z_{sink} \quad (8)$$

The IGBT and diode thermal impedances are in parallel. The equivalent thermal impedance of thermal paste is related to the effective area and thickness of the selected thermal paste,

$$R_{Paste} = \rho \cdot \frac{\theta}{A} \quad (9)$$

where ρ is the resistivity of the selected thermal paste, θ is the thickness of thermal paste, A is the area of thermal paste. The detailed parameters of the thermal model are summarized in Table I [21]. The thermal model in Table I assumes that the diode and IGBT chip are embedded in the same module package such as TO-247. The IGBT/diode module is attached to the heat sink through the thermal paste with the same area of the package. The PV inverter power loss characteristics are summarized in Table II [22].

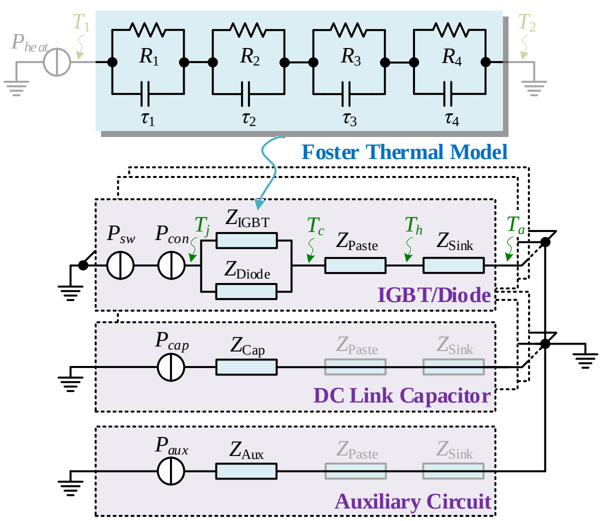

Fig. 3. Detailed thermal model of PV inverter.

IV. Lifetime Estimation of PV Inverter

The lifetime estimation for a PV inverter involves in-depth knowledge of multiple subjects. To simplify the analysis, the lifetime estimation of an IGBT will be used as the lifetime estimation of a PV inverter. The lifetime model of IGBTs can be formulated as follows [23],

$$N_f = A \times (\Delta T_{junc})^{\alpha} \times (ar)^{\beta_1 \Delta T_{junc} + \beta_0} \times \left[\frac{C + (t_{on})^{\gamma}}{C+1}\right] \times \exp\left(\frac{E_a}{k_b \times T_{junc}}\right) \times f_d \quad (10)$$

where N_f is the number of cycles to failure. This parameter indicates that a new IGBT module is going to fail after N_f cycles of use for a given operating condition. ΔT_{junc} is the temperature variation in time period of t_{on}. t_{on} is the thermal cycle period, which is the same as the electrical line period [24]. ΔT_{junc} is estimated by an empirical value [24],

$$\Delta T_{junc} = 0.2 \times (T_{junc} - T_{amb}) \quad (11)$$

The other parameters are given in Table III [23].

From (6), (8), (10) and (11), the PV inverter lifetime is related to ambient temperature and the apparent power

$$S = \sqrt{P^2 + Q^2} \quad (13)$$

$$N_f = f(P, Q, T_{amb}) \quad (14)$$

Fig. 5 shows the normalized lifetime (NLT) given an ambient temperature of 25 °C. The active power is curtailed when reactive power increases and the apparent power reaches to the nominal rating. If the active power output is high, the estimated lifetime does not decrease much when reactive power increases. The lifetime shortening effect is fixed once the PV inverter falls into the active power curtailment zone because it is operating at its maximum apparent power.

V. Marginal Cost and Supply Curve

The PV inverter supply curve represents the marginal cost of the PV inverter to provide reactive power. The cost to PV inverters for providing reactive power includes: a) loss of revenue (LoR) due to active power curtailment (if any), and b) wear-and-tear cost of the PV inverter. The cost to LoR of this paper follows [12]. The cost to power loss can be formulated as

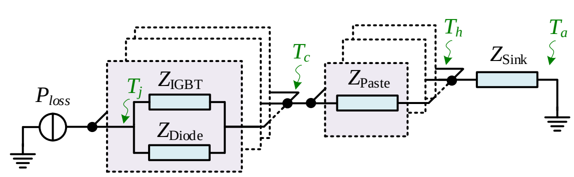

Fig. 4. Simplified PV inverter thermal model.

$$T_{junc}^i = (P_{sw}^i + P_{con}^i) Z_{sw}^{eq} + T_{amb} = (P_{sw}^i + P_{con}^i)(Z_{IGBT}^i \parallel Z_{Diode}^i + Z_{Paste}^i + Z_{Sink}^i) + T_{amb} = (P_{sw}^i + P_{con}^i) \left(\begin{array}{c} \sum_j^m R_j^{IGBT} \left(1 - e^{-\frac{t}{\tau_j^{IGBT}}}\right) \parallel \sum_j^m R_j^{Diode} \left(1 - e^{-\frac{t}{\tau_j^{Diode}}}\right) \\ + \sum_j^m R_j^{Paste} \left(1 - e^{-\frac{t}{\tau_j^{Paste}}}\right) + \sum_j^m R_j^{Sink} \left(1 - e^{-\frac{t}{\tau_j^{Sink}}}\right) \end{array} \right) + T_{amb} \quad (7)$$

TABLE I. KEY PARAMETERS OF PV INVERTER'S THERMAL MODEL [21]

	Thermal Resistance (K/kW)				Thermal Capacitance ($\times 10^{-3}$ s)				Count
IGBT	$R_1 = 5.24$	$R_2 = 1.54$	$R_3 = 1.57$	$R_4 = 0.145$	$\tau_1 = 151$	$\tau_2 = 24.9$	$\tau_3 = 3.86$	$\tau_4 = 0.661$	6
Diode	$R_1 = 10.4$	$R_2 = 3.19$	$R_3 = 3.08$	$R_4 = 0.299$	$\tau_1 = 151$	$\tau_2 = 24.9$	$\tau_3 = 3.86$	$\tau_4 = 0.661$	6
Thermal Paste	$\rho = 142$ K·cm/W	$\theta = 50.8$ µm	$A = 5.9$ cm^2		$\tau = 1000$				6
Heat Sink	$R = 500$				$\tau = 1000$				1

TABLE II. PV INVERTER POWER LOSS CHARACTERISTICS [22]

	k_2	k_1	k_3	P_{out}	R_{eq}	Model
Inverter 1	1.471×10^{-5}	0.03733	18.831	2.5 kW	0.5528 K/W	SMA SWR-2500U

TABLE III. PARAMETERS OF THE LIFETIME MODEL OF AN IGBT MODULE [23]

Parameter	Value	Experimental condition
A	3.4368×10^{14}	
α	-4.923	$5\ \text{K} \le \Delta T_{junc} \le 80\ \text{K}$
β_1	9.012×10^{-3}	
β_0	1.942	$0.19 \le ar \le 0.42$
C	1.434	
γ	-1.208	$0.07\ \text{s} \le t_{on} \le 63\ \text{s}$
f_d	0.6204	
E_a	0.06606 eV	$32.5\ °\text{C} \le T_{junc} \le 122\ °\text{C}$
k_B	8.6173324×10^{-5} eV/K	

$$C_{loss} = \text{ET} \times P_{loss}^{Qreq}\ , \quad (15)$$

where P_{loss}^{Qreq} is the power loss for the reactive power production, ET is the electricity tariff. NLT is selected as an index to indicate the lifetime shortening effect of reactive power for the PV inverters. NLT = 1 when the lifetime shortening effect is not present. NLT decreases towards zero when the lifetime shortening effect increases.

Modify (15) to consider NLT,

$$C_{loss}^{\text{NLT}} = C_{loss}/\text{NLT}\ . \quad (16)$$

The total reactive power cost is calculated as follows,

$$C_{total}^{Q} = C_{LoR} + C_{loss}^{NLT}\ . \quad (17)$$

Differentiate (17) with respect to the requested reactive power to compute the marginal cost of reactive power.

$$\text{MC}^{Q} = \frac{dC_{total}^{Q}}{dQ_{req}}\ , \quad (18)$$

where, MC^{Q} is the marginal cost to PV inverter for providing reactive power, dC^{Q}_{total} is the first order differentiation of cost of producing reactive power, dQ_{req} is the first order differentiation of requested reactive power. The marginal cost for providing reactive power is the supply curve for the PV inverter.

VI. CASE STUDY

To verify the proposed marginal cost considering NLT, a 24-hour simulation is conducted. The demand curves from customers are compared with the supply curves to determine the cleared price. The reactive power demand curve of this paper follows [12]. A sampled 24-hour MPPT profile from a typical PV inverter is fed into the simulation. After the market is cleared, the cleared price will be sent from TES to distributed controllers to dispatch the PV inverter based on its price curve. Fig. 6 shows the MPPT profile and the actual active power output of the PV inverter using the marginal cost model with and without NLT algorithm. The active power production has no difference between these two cases.

Fig. 7 shows that the actual reactive power output of the PV inverter using the marginal cost model with and without NLT. The actual reactive power generated by the PV inverter using NLT algorithms is smaller than the one without the NLT algorithm. Fig. 8 shows the estimated lifetime usage of the PV inverter in this case study. The PV inverter uses 0.15% of its lifetime with the NLT algorithm, whereas it uses 0.35% of its lifetime without the NLT algorithm. This case study demonstrates that the proposed marginal cost model can effectively reduce the life-shortening effect of the reactive power production.

VII. CONCLUSION

This paper discusses the lifetime-shortening effect of PV inverters when providing ancillary services. The lifetime estimation shows that the lifetime-shortening effect of reactive power correlates with active power and ambient temperature. Based on the lifetime estimation, an improved marginal cost model of reactive power is proposed for PV inverters. The

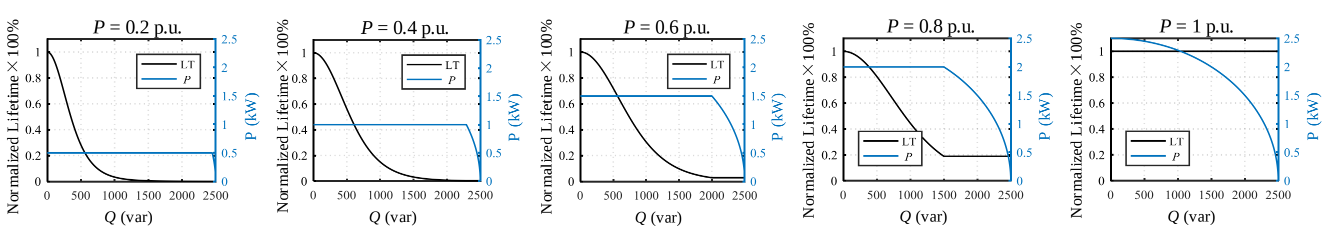

(a) (b) (c) (d) (e)

Fig. 5. Normalized lifetime of a PV inverter by giving T_{amb} = 25 °C. (a) P = 0.2 p.u.; (b) P = 0.4 p.u.; (c) P = 0.6 p.u.; (d) P = 0.8 p.u.; (e) P = 1.0 p.u.

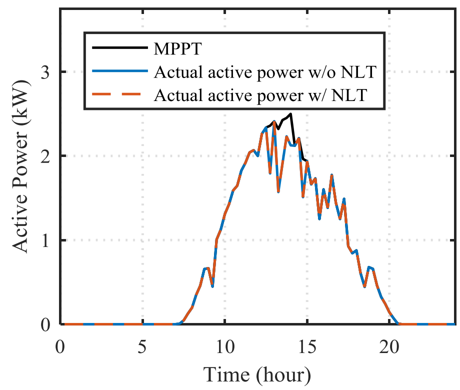

Fig. 6. MPPT profile and the actual active power output of the PV inverter using supply curve with and without NLT.

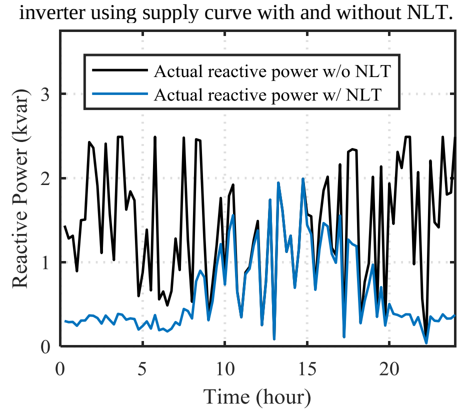

Fig. 7. Actual reactive power output of the PV inverter using supply curve with and without NLT.

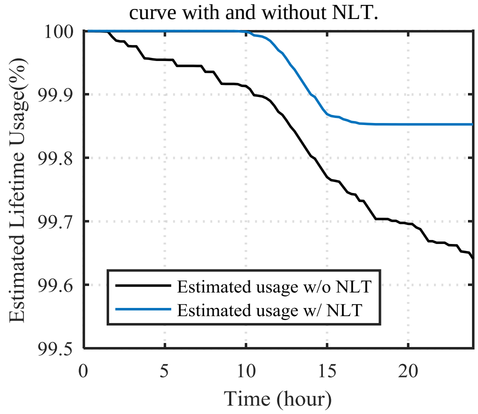

Fig. 8. Estimated lifetime usage of PV inverter.

improved marginal cost gives a quantitative consideration of the thermal stress of the reactive power for the PV inverter given the conditions of active power and ambient temperature. The proposed model is validated by a simulation case study. The case study shows that the proposed marginal cost model can effectively avoid excessive thermal stress on the PV inverter.

REFERENCES

[1] M. Woodhouse *et al.*, "On the path to sun shot: the role of advancements in solar photovoltaic efficiency, reliability, and costs," *Natl. Renew. Energy Lab.*, NREL/TP-6A20-65872. May, 2016.

[2] A. Golnas, "PV system reliability: An operator's perspective," *IEEE J. Photovoltaics*, vol. 3, no. 1, pp. 416–421, 2013.

[3] L. M. Moore and H. N. Post, "Five years of operating experience at a large, utility-scale photovoltaic generating plant," *Prog. Photovoltaics Res. Appl.*, vol. 16, pp. 249–259, 2008.

[4] S. Yang, A. Bryant, P. Mawby, D. Xiang, L. Ran, and P. Tavner, "An industry-based survey of reliability in power electronic converters," *IEEE Trans. Ind. Appl.*, vol. 47, no. 3, pp. 1441–1451, 2011.

[5] H. Wang, K. Ma, and F. Blaabjerg, "Design for reliability of power electronic systems," *Annu. Conf. IEEE Ind. Electron. Soc.*, pp. 33–44, 2012.

[6] M. Andresen, G. Buticchi, and M. Liserre, "Thermal stress analysis and MPPT optimization of photovoltaic systems," *IEEE Trans. Ind. Electron.*, vol. 63, no. 8, pp. 4889–4898, 2016.

[7] Y. Yang, H. Wang, and F. Blaabjerg, "Improved reliability of single-phase PV inverters by limiting the maximum feed-in power," *IEEE Energy Convers. Congr. Expo.*, pp. 128–135, 2014.

[8] Y. Yang, E. Koutroulis, A. Sangwongwanich, and F. Blaabjerg, "Pursuing photovoltaic cost-effectiveness: absolute active power control offers hope in single-phase PV systems," *IEEE Ind. Appl. Mag.*, vol. 23, no. 5, pp. 40–49, 2017.

[9] Victron Energy, "Technical notes on output rating, operating temperature and efficiency," 2018. [Online]. Available: https://www.victronenergy.com/upload/documents/Output-rating-operating-temperature-and-efficiency.pdf

[10] L. Guangzhou Sanjing Electric CO., "Sunfree solar inverter datasheet." [Online]. Availale: https://www.lizard.cl/_PDF/invh400048/Sunfree_Hybrid_Solar_Inerter_4K5K.pdf

[11] Solaredge, "Temperature de-rating - technical note (Europe & APAC)," 2019. [Online]. Available: https://www.solaredge.com/sites/default/files/se-temperature-derating-note-na.pdf

[12] J. Alam, R. Melton, A. Somani, and T. DcDermott, "Transactive approach for engaging distribution network assets for voltage management in southern california edison distribution feeders," Pacific Northwest National Laboratory (PNNL), Richland, WA, United States, Tech. Rep., 2018.

[13] B. P. Bhattarai *et al.* "Enhancing distribution system resiliency through a novel transactive energy systems framework," *IEEE Power and Energy Society General Meeting*, Atlanta, GA, 2019.

[14] J. Li, C. Zhang, Z. Xu, J. Wang, J. Zhao, and Y. J. A. Zhang, "Distributed transactive energy trading framework in distribution networks," *IEEE Trans. Power Syst.*, vol. 33, no. 6, pp. 7215–7227, 2018.

[15] Z. Liu, Q. Wu, S. Huang, and H. Zhao, "Transactive energy: A review of state of the art and implementation," *IEEE PowerTech*, pp. 1–6, 2017.

[16] Z. Liu, Q. Wu, K. Ma, M. Shahidehpour, Y. Xue, and S. Huang, "Two-stage optimal scheduling of electric vehicle charging based on transactive control," *IEEE Trans. Smart Grid*, vol. 10, no. 3, pp. 2948–2958, 2019.

[17] A. Anurag, Y. Yang, and F. Blaabjerg, "Reliability analysis of single-phase PV inverters with reactive power injection at night considering mission profiles," *IEEE Energy Convers. Congr. Expo.*, pp. 2132–2139, 2015.

[18] A. Anurag, Y. Yang, and F. Blaabjerg, "Thermal performance and reliability analysis of single-phase PV inverters with reactive power injection outside feed-in operating hours," *IEEE J. Emerg. Sel. Top. Power Electron.*, vol. 3, no. 4, pp. 870–880, 2015.

[19] Texas Instrument, "MOSFET power losses and how they affect power-supply efficiency," AAJ 1Q 2016. [Online]. Available: http://www.ti.com/lit/an/slyt664/slyt664.pdf

[20] Semikron, "Thermal resistance of IGBT modules - specification and modelling," 2014. [Online]. Available: https://www.semikron.com/dl/service-support/downloads/download/semikron-application-note-thermal-resistances-of-igbt-modules-en-2014-11-30-rev-01/

[21] Hitachi Power Semiconductor Device, "Thermal equivalent model of IGBT modules," 2015. [Online]. Available: http://www.hitachi-power-semiconductor-device.co.jp/en/products/igbt/pdf/thermal_model.pdf

[22] D. L. King, S. Gonzalez, G. M. Galbraith, and W. E. Boyson, "Performance model for grid-connected photovoltaic inverters," Albuquerque, New Mexico, SAND2007-5036, 2007.

[23] A. Sangwongwanich, Y. Yang, D. Sera, and F. Blaabjerg, "Lifetime evaluation of grid-connected PV inverters considering panel degradation rates and installation sites," *IEEE Trans. Power Electron.*, vol. 33, no. 2, pp. 1225–1236, 2018.

[24] Z. Wang, "Real-time internal temperature estimation and health monitoring for IGBT modules," Ph.D. dissertation, Dept. Electr., Comput. Eng., Univ. Nebraska-Lincoln, 2017.